RECEIVE SENSITIVITY ANALYSIS OF CMUT FOR UNDERWATER ACOUSTIC COMMUNICATION

Submitted by
Muhammad Omer Asim

Submitted to the Graduate School of Engineering and Natural Sciences
in partial fulfillment of the requirements for the degree of Master of Science
SABANCI UNIVERSITY
Summer 2018

RECEIVE SENSITIVITY ANALYSIS OF CMUT FOR UNDERWATER ACOUSTIC COMMUNICATION

APPROVED BY:

Associate Professor, Dr. Ayhan Bozkurt
(Thesis Supervisor) .....

Associate Professor, Dr. Ahmet Onat .....

Associate Professor, Dr. Göksenin Yaralioğlu .....

DATE OF APPROVAL: 31/07/18

ABSTRACT

RECEIVE SENSITIVITY ANALYSIS OF CMUT FOR UNDERWATER ACOUSTIC COMMUNICATION

Muhammad Omer Asim

FENS, MSc Thesis, 2018

Supervisor: Assoc. Prof. Dr. Ayhan Bozkurt

Keywords: Capacitive micromachined ultrasonic transducer (CMUT), Finite element model (FEM), Receive Sensitivity, Hydrophone

The underwater communication among autonomous underwater robots, working in swarm, need to be reliable and accurate. The communication and sensing transducers used on the robots must withstand the harsh underwater environment.

For catering such necessities, the transducers ought to be light weight, flexible and mountable on the robot surfaces. In this work a CMUT with small size, higher sensitivity and lower power consumption is suggested as an alternative to the conventional communication devices. The CMUT is designed, analyzed and tested as an underwater acoustic communication device in receive mode.

Receive sensitivity analysis is performed using finite element analysis. The fabricated device is tested in lab environment and the results showed consistency to the commercial devices.

ÖZET

SUALTI AKUSTİK İLETİŞİMİ İÇİN CMUT'IN DUYARLILIK ANALİZİ

Muhammad Omer Asim
FENS, Yüksek Lisans Tezi, 2018
Danışman: Doç. Dr. Ayhan Bozkurt

Anahtar kelimeler: Kapasitif mikromaktif ultrasonik güç çevirici (CMUT), Sonlu eleman modeli (FEM), Hassasiyet Alma, Hidrofon

Sualtında çalışan su altı robotları arasındaki sualtı iletişiminin güvenilir ve doğru olması gerekir. Robotlar üzerinde kullanılan iletişim ve algılama dönüştürücüleri, sert su altı ortamına dayanmalıdır.

Bu tür ihtiyaçların karşılanması için, dönüştürücüler, robot yüzeylerinde hafif, esnek ve monte edilebilir olmalıdır. Bu çalışmada, geleneksel iletişim cihazlarına alternatif olarak küçük boyutlu, daha yüksek hassasiyet ve daha düşük güç tüketimine sahip bir CMUT önerilmektedir. CMUT, alım modunda bir sualtı akustik iletişim cihazı olarak tasarlanmış, analiz edilmiş ve test edilmiştir.

Alma duyarlılık analizi sonlu elemanlar analizi kullanılarak gerçekleştirilir. Üretilen cihaz laboratuar ortamında test edildi ve sonuçlar ticari cihazlara tutarlılık gösterdi.

In dedication to my parents for making me who I am and to my wife and daughter for their love and support!

ACKNOWLEDGEMENTS

I would like to express my deepest appreciation to my supervisor Ayhan Bozkurt for his patience, encouragement and guidance.

I am grateful to him for giving me an opportunity to be a part of SU Acoustic group, I could not have imagined a better advisor and mentor. Without his guidance and persistent help this thesis would not have been possible.

My sincere gratitude is extended to my committee members, Assoc. Prof. Dr. Ahmet Onat and Assoc. Prof. Dr. Göksenin Yaralıoğlu for their valuable time, review and comments on the thesis.

Special thanks to Mansoor Ahmad, he is the reason I joined SU, thanks a lot for your guidance, help and support. I owe you a lot mate. During the course of this work, the constant support and advice of colleagues Mansoor Ahmad, Dr. Omid Farhanieh and Dr. Rupak Bardhan Roy made my stay and work pleasurable. Mansoor's fabrication skills and Omid's tips and instructions were of great help.

I would like to extend my appreciation to family especially my parents for their constant support, prayers and encouragement.

Foremostly, I would like to thank my wife Jaweria and daughter Nabiha for their endless love and patience. Their limitless tolerance, encouragement and care made everything about me possible. Thank you for being there for me.

Table of Contents

List of Figures

List of Tables

List of Equations

CHAPTER 1

INTRODUCTION:

What we cannot see, intrigues us. Nature has covered about three fourths of our Planets' surface with water, beneath which there may lie secrets to a whole new universe that is yet to be explored. As one of mankind's most primitive characteristic, it is captivating. From the beginning of times we have strived to seek answers to the complexity of this hidden universe of possibilities. Leonardo Da Vinci was the first to come up with the idea of using sound waves as a medium for under water communication. As a verification to his hypothesis, he successfully detected a distant ship by using an extended duct underwater. [1].

During the second World war, with all the unfortunate destruction, came the realization that underwater communication was going to be imperative for naval warfare in the coming times. As a result, one of the earliest underwater telephone was developed in 1945 to ensure communication with submarines. [1] Luckily, we live in the era in which technological advancement has equipped us with the tools to explore under-water communication with much greater efficiency and effectiveness by using compact, power efficient, miniaturized and accurate devices than before.

Demands for better and reliable underwater communications have been increasing lately because of the ongoing expansion in human trans-medium activities including coastline/border surveillance, underwater environmental observation, off-shore oil/gas field exploration, oceanographic data gathering and controlling autonomous underwater vehicles (AUVs) and remotely operated vehicles (ROVs). [2]

Potential communication beneath sea level has been possible because of three types of waves namely optical, electromagnetic and acoustic waves. Optical waves can reach up to 60m in limpid waters while in murky and muddy waters, the backscattering occurs limiting its range even further. Luckily, acoustic waves have no such shortcoming in harsh conditions. [3].

When it comes to propagation in shallow fresh water Electromagnetic (EM) waves may outperform acoustic waves as they are faster and are less prone to reflections and absorptions as indicated by [4] But in most practical environments like sea water, EM waves fail to compete with acoustic waves. The conductivity in sea water causes high attenuation for EM waves. [5].

1.1: Advancement in Underwater Communication:

With the advancement and progress of VLSI technology, Underwater acoustic communication-UWAC tools and system saw a rapid growth. Development of power efficient DSPs has enhanced the working range and data throughput of underwater acoustic communication systems. Acoustically controlled robots have replaced divers; data links between the surface and the deepest of trenches has been established; and communication among parallel distances of more than 200 kilometers has been verified. [6].

The scope of underwater communication systems continues to nurture for both commercial and military applications, providing enhanced and robust communication between submarines and unmanned, or autonomous underwater vehicles (UUVs, AUVs). Underwater vehicles can get rid of cables and develop self-awareness by sharing control and telemetry data enabling them to work efficiently in swarms.

1.2: SWARM:

Recently swarm robotics phenomenon has been introduced; and is gaining a lot of importance especially for underwater acoustics communication. As the name suggests swarm robotics is when many robots work together in a team to accomplish a distinct job. Swarms might have just been brought into light but are not lately invented; nature has observed various creatures working in swarm groups since thousands of years, for instance ants, honey bees and dolphins etc.

By employing several robots in a group to accomplish a certain task, Swarm robotics has brought along many advantages, such as efficiency and enhanced range of operations. Overall system reliability and effectiveness is achieved by reducing the time and efforts to complete any given task as compared to the single robot. Moreover, replacement and maintenance of a single unit from the swarm is more practical rather than replacing a single robot working outside the swarm that is solely responsible for everything related to the assigned project. Among the popular applications of swarm robotics are harbor surveillance, mapping and surveying, ships/boats hull inspection, mining of underwater natural resources and study of several oceanographic phenomenon such as fish migration and sea vegetation growth. [7].

1.2.1: SWARMS Communication:

Swarms communication can be divided into two main categories namely direct and indirect. Direct communication is similar to two individuals or in this particular case two robots from the swarm conversing with one another, this can either be wired or unwired. For indirect form of communication, the environment is altered according to the communication needs to deliver a message from one element to another within a

swarm. This type is not preferred; as it can be slow, distracted by excessive noise and hard to interpret for the robots.

Swarms can either be used on land or in water; with the assistance of omnidirectional antennas and radio frequencies, communication is possible on land however this is not the case when it comes to underwater communication. Underwater is the harshest environment for establishing communication.

The high frequency radio waves are easily absorbed by water severely limiting the range of RF transceivers, the swarm robots must stay adjacent and close to one another in order to communicate effectively. Staying in such a proximity can result in collision and failure of many other algorithms. Several different methods have been further introduced to overcome this problem. One of them is using flashes of light to communicate with the robots but this solution eventually flops in murky waters.

Another eminent technique brought to practice to solve the communication problem is the use of tethers, being the fastest form of communication among swarms so far. The only limitation that occurs here is that the robot is confined just to the length of the tether and the tether wire can easily get tangled. [8].

Due to these restrictions that water enforces on communication, acoustic communication is preferred underwater. The main drawbacks of end-to-end delay and signal attenuation have been curbed by establishing successful short-range underwater acoustic communication systems, for example a 500m end-to-end propagation will take approximately 0.3 sec. Lower attenuation means lesser transmitter power requirement, reducing the size and power of batteries installed on AUVs; the costly recharge and replacement of batters is also avoided. At short range, the effects of temperature, salinity and ambient pressure on communication is further reduced. [9].

CHAPTER 2

ACOUSTIC TRANSDUCERS:

Acoustic waves traditionally produced by a vibrating element- a transducer, outperform optical and EM waves for under water communication. A Transducers converts electrical energy into sound waves when acting as a transmitter and converts the received sound waves into electrical pulses when acting as a receiver.

2.1: Comparison (PZTs vs. MUTs)

Conventionally, Transducer can be a PZT- Lead Zirconate Titanate and Piezo based composite device or a MUT- Micromachined Ultrasonic Transducer device.

2.1.1: Piezoelectric Transducers:

Piezoelectric effect was first discovered by none other than the French brothers Jacques and Pierre Curie in 1880 when they found out that putting pressure on certain materials (crystals, ceramics and even bone) created electricity. These materials develop an electrostatic potential when subjected to pressure. The name piezoelectricity came from a Greek word “piezen” that means “squeeze”. For most of the underwater applications piezoelectric transducers made with Lead Zirconate Titanate are mostly preferred over any other transducer. Apart from being economic these transducers are efficient and flexible. Piezoelectricity is used for the conversion of electrical signals to mechanical vibrations called the transmit mode and again from mechanical vibrations to electrical signals called the receive mode. Most of the PZTs today use piezoelectric ceramic which can be cut into numerous different shapes in order to create different wave modes. These can be effectively employed for both; low temperatures and high voltages.

There are certain substances that naturally possess the piezoelectric properties, strongest among the whole collection discovered are quartz and Rochelle salt. However, synthetic piezoelectric materials can also be manufactured by using either polycrystalline ceramics or synthetic polymers. Powder of the desired polycrystalline material is pressed to form the required shape which is commonly rectangular or circular. Afterwards these parts are cooked in a kiln on extremely high temperatures. Furthermore, to gain the required mechanical or frequency tolerance, these parts need

some mandatory grinding or lapping. Typically, silver electrodes are later applied to allow the application of electrostatic potential. After completion of all the above steps the ceramic has now gained uniformity which means it's isotropic, composed of many crystals randomly oriented where each crystal cell is now behaving like a dipole. The ceramic is made piezoelectric by the process of polling where these dipoles are aligned parallel to the field by applying a strong DC field at a very high temperature ultimately making the ceramic anisotropic.

The transducer will start vibrating at the applied frequency of alternating current across its electrodes. Conversely, the alternating current voltage will appear across the transducers electrodes if it is subjected to vibrations.

With all the advantages, Piezoelectric ultrasonic transducers based on PZT has had its limitations, low operational efficiency, Inefficient coupling to air/water, matching and backing layers requirement, too large for consumer electronics, difficulty in processing two-dimensional arrays, and narrow operating bandwidth makes it unfit for modern acoustic transducer requirements. [10].

2.1.2: Micromachined Ultrasonic Transducers:

About three decades ago, with the advent of micro-machining technologies, MUT- Micro Machined Ultrasonic Transducers came into existence. Micro machining permits fabrication of electrostatically driven membranes repeatedly in forms of arrays with ease of integration with CMOS technology. [11].

MUTs enjoy the intrinsic advantages of microfabrication, which include low cost, array fabrication, and the possibility to integrate electronics producing system in package or system on chip or even multi-chip modules.

The use of micro machining fabrication technology allows detection of acoustic signals by the silicon piezo-resistivity or capacitance improving the imaging resolution. [12].

Currently, MUTs can be either pMUTs- piezo Micromachined Ultrasonic Transducers first envisioned in 1983 [13] or cMUTs- capacitive Micromachined Ultrasonic Transducer invented by [14].

For coupling applications, both CMUTs and pMUTs offer a better matching to the load compared with the typical piezoelectric transducers eliminating the need of impedance matching and backing and therefore they have a larger intrinsic bandwidth.

2.2: Piezo Micromachined Ultrasonic Transducers:

PMUT uses piezo in flexional bimorph creating large piezoelectric actuations. Their small element size, low power consumption and ease of fabrication of large arrays for imaging and communication applications achieved by MEMS fabrication process is

rapidly making them a good replacement for conventional bulk piezoelectric transducers. [15].

However, their relatively narrow bandwidth, difficult and expensive fabrication process involving sputtering of piezoelectric material and impedance mismatch with the acoustic impedance of air or surrounding medium make them second to CMUTs. At present pMUTs are in a very initial stage of development and the potential benefits over the CMUTs are still to be established.

2.3: Capacitive Micro machined Ultrasound Transducers:

CMUTs are electro-acoustic MEMS transducers operating at ultrasonic frequencies (MHz) with broader frequency response, higher reception sensitivity, and higher thermal efficiency.

CMUTs have been emphasized here as they have shown good electroacoustic characteristics, which parallel, or even exceed, those of conventional piezoelectric transducers making them a strong replacement contender to the piezo based transducers.

Up till recently an ultrasonic device based on piezo electric effect has been the core device in ultrasonic technologies, and these technologies have been greatly affected by the range, diversity and performance of these piezo devices. With the extended use of ultrasonic transducers mainly based on piezo effect, conventional piezo transducers and PMUTs, their limitations and complications have slowly but surely become apparent. The acoustic impedance mismatch between piezoelectric materials and air, water and human tissues is one of the most damaging limitation of piezo devices, degrading the sound pressure levels at the transmission and reception interfaces. Thus, critically influences the transmission and reception sensitivity, the axial resolution, reduces the coupling coefficient (k) and badly effect the bandwidth and energy of the system. Adding a matching layer between the piezoelectric ceramic and the media of operation usually solves the mismatch issue but this method leads to other problems such as loss of bandwidth, increased system complexity and higher production cost. [16].

With rapid development in MEMS-Micro Electro Mechanical Systems fabrication technologies like micromachining and photolithography the acoustic transducer development has seen a rapid growth. CMUTs fully utilizes the advantages offered by micro fabrication that piezo devices failed to utilize. Silicon microfabrication lead to higher suitability for electronic integration (monolithic or hybrid), making die- and wafer-level packaging processes adoptable; lead-free and cost effective,

Large arrays, batch production and a better impedance match between device and surrounding media was realized producing devices with broad capacitance coverage and high electromechanical conversion efficiency. [17], [18], [19].

2.3.1: Conventional CMUT:

The simplest CMUT is a thin membrane stretched upon a back electrode forming a cavity. Two electrodes with cavity in between act like a capacitor which can be charged by applying a DC voltage. When an impinging acoustic wave strikes the membrane, it bends, changing the capacitance and creating an AC voltage at the electrodes of the device. The magnitude of this AC voltage is proportional with the intensity of the striking acoustic wave. Similarly, the inverse is also true, with application of AC voltage an acoustic wave corresponding with the frequency of applied signal can be generated. Figure 1 shows schematic of the simplest CMUT.

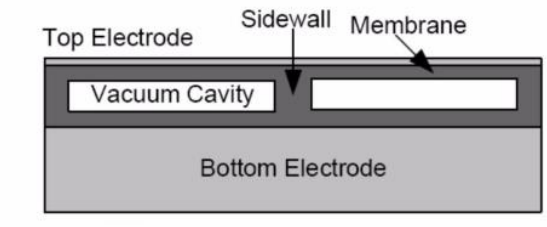

Figure 1: Simplest CMUT

2.3.2: Working:

A thin plate vibrating under the influence of electrostatic forces is the primary working principle of the CMUT. Other devices like microphones and loud speaker use the same fundamental concept.

Under the influence of the applied DC voltage the two electrodes attract each other but the residing stress in the membrane opposes this attraction force. If alternating voltage is applied, the membrane starts vibrating. Care should be taken while biasing the device as the applied DC voltage should not exceed the pull in voltage otherwise the membrane will collapse. Hence, the device should be operated at less than the collapse voltage. The figure 2 shows the device in operation.

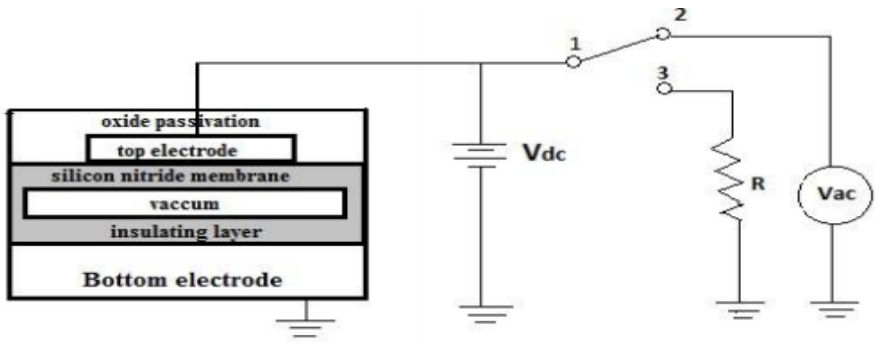

Figure 2: CMUT working

2.3.3: Conventional Fabrication Processes:

The CMUT fabrication process starts with a low-resistivity silicon wafer. The silicon wafer can be heavily doped to achieve high conductivity at the surface, eliminating the need for bottom electrode of the device. A second membrane is placed over the first one with side wall supports, creating a vacuum. The top substrate can also be heavily doped like the bottom electrode, or it can be sputtered or evaporated with metal to form the top electrode. Similarly, the bottom electrode can also be formed in case the bottom substrate is not doped.

The fabrication processes can be broadly segregated into surface micromachining process using sacrificial layer and wafer bonding process. [20], [23].

For releasing the membrane and removing the sacrificial layer, small under holes are etched during surface micromachining processes, causing the fill factor of the device to degrade. [21]. Another challenging task is drying the cavity after wet etching, as it may cause stiction resulting in membrane collapse.

Owing to varying factors like layer width, sacrificial material choice, etchant selection, release hole positioning and size and structure of membrane, achieving device fabrication preciseness, performance and repeatability is demanding. Optimization of various design parameters remain a tradeoff effecting the reliability of the device.

On the contrary, wafer bonding simplifies the fabrication process by covering the predefined cavities by an accurate mechanical cover in a single bounding step. Wafer bonding is devoid of sacrificial layers, effectively lowering the fabrication steps and increasing device active area by not requiring release holes.

The active region and diameter of the device are defined by patterning and etching before the bonding step, hence fabrication repeatability and reliability is attained by controlling the width, uniformity and mechanical properties of vibrating plate. [21]. Single crystal silicon membranes with lower mechanical defects and internal stresses add to the advantages of the process especially during large arrays formation. [22].

During conventional wafer bonding, the wafer surface unevenness limits the yield of the device, the smoothness can be achieved by either purchasing expensive SOI wafers or employing CMP treatment. Furthermore, CMOS compatibility cannot be achieved due to annealing process which typically ranges from 800 °C–1100 °C. A CMOS suited process, with temperature under 400 °C, can allow fabrication of CMUTs directly on integrated circuits (ICs) enhancing device efficiency and compactness.

Among various wafer bonding techniques by adhesive bonding, fusion bonding and anodic bonding are prevalent. Thermocompression bonding also referred as diffusion bonding is like solid-state wielding. By applying pressure and temperature simultaneously while keeping the two metals in close proximity, allows the migration of atoms among lattice sites. This migration of atoms joins the crossing points together forming a bond between the boundaries. Among the three, Copper-Cu, Gold-Au and

Aluminium-Al, most widely used metals for thermocompression bonding, Au requires the lowest process temperature. Unlike the other two Au doesn't form oxides and maintainability and handling of gold is also easier. [24].

Before the design phase, certain aspects of the device were pre-decided. CMUT devices are intended for communication among marine vehicles working underwater. Hence, devices need to be robust enough to withstand the unfavorable sea environment. To bear the varying underwater hydrostatic pressure that doubles with every 10 meters depth the thicker membrane will be used.

CHAPTER 3

DESIGN:

Designing CMUTs is a continual improvement process which is yet to be perfected, and new CMUT design, theory and methods are still being studied and finalized. The parameters like cavity height, membrane thickness and shape, electrode dimensions and placement all contribute towards the design of CMUT and combine to define the working principle, operating frequency, collapse voltage and other working parameters.

The geometrical specifications of the membrane and the gap are responsible for the performance and frequency characteristics of the CMUTs. Hydrophones sensitivity is the measure of voltage produced across its face per unit of hydrostatic pressure. The mechanical sensitivity [V/Pa] of a circular shaped sensing diaphragm for an underwater hydrophone can be given

$$S = \frac{a^2}{8\delta t^3}$$

Equation 1 :Mechanical sensitivity of a circular sensing diaphragm used for underwater hydrophone

where diaphragm radius is denoted by ‘a’, hydrophone’s diaphragm residual stress is denoted by δ, and the thickness of hydrophones diaphragm is ‘t’. The equation clearly indicates that increasing the diaphragm area can improve the mechanical sensitivity of the hydrophone.

To withstand the varying underwater hydrostatic pressure, which can easily collapse the structure by over-deflecting thin membrane, a large membrane of 525um is used. By employing wafer bonding technique thickness of 525um is achieved by using a highly doped, low resistivity Silicon wafer as the membrane. To prevent an electrical break down by ohmic contact between top and bottom electrode; a thick insulation layer of thermally grown oxide is used. Keeping in view the typical value of dielectric strength (800-1000 V/um) for thermally grown oxide, the oxide thickness is kept at 1um to maintain high operating voltages. [25]

For effective receive mode operation the gap is kept low to attain high sensitivity, while efficient transmission requires enough space for membrane displacement to produce higher output pressure. Hence, the optimum cavity height design is a trade-off between reception sensitivity, dependent on electrical field intensity and higher transmission dependent upon generated output pressure. After through deliberation of these requirements, for a passive listening device, the optimal cavity height is established to be 1 μm.

As lower frequency acoustic wave can propagate to farther distances, the device under consideration is designed to operate around 200kHz as a receiver for underwater communication applications. The CMUTs operating point is greatly affected by underwater hydrostatic pressure, hence the device under consideration is designed for operating at 0-5 meters depth. [26].

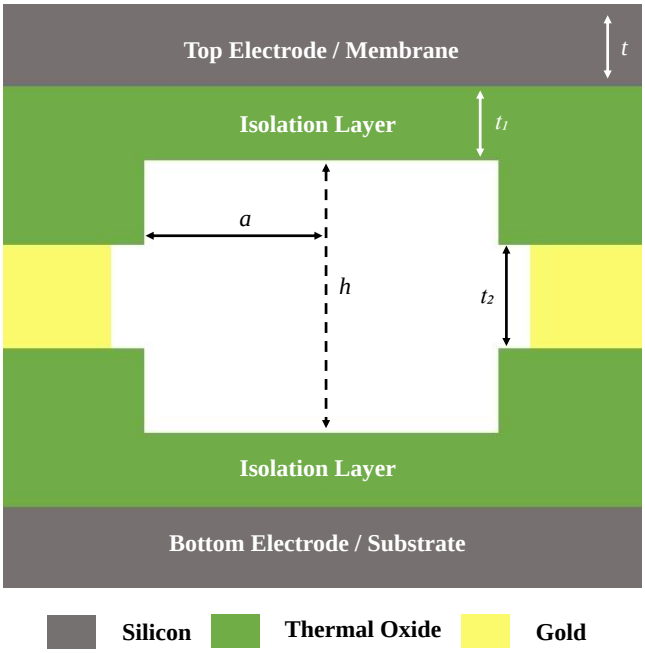

Figure 3: Parameters for CMUTs

A cross-sectional view of CMUT device is depicted in figure 3, describing the physical parameters such radius 'a', membrane thickness 't', cavity height 'h' and oxide thickness 't_2'. The bottom and top electrode along with the posts are also shown.

3.1: Simulations for CMUTs Characterization:

A static analysis was performed for the collapse voltage determination. Resonant frequencies were calculated by carrying out harmonic analysis. A pre-stressed harmonic analysis was used to determine the effects of DC bias on the resonant frequency. Finally, a transient analysis was performed to figure out the receive sensitivity of the CMUT working underwater. The material properties used in the simulations are listed in Table II. The corresponding CMUTs characteristics such as collapse voltage, the resonant frequencies and the receive sensitivity analysis for the said parameters are calculated and optimized using ANSYS finite element analysis software.

3.1.2: Collapse Voltage:

CMUTs are usually operated with a high DC biased to increase the membrane deflection; this deflection increases the acoustic output of the device by lowering the distance between the electrodes. Unfortunately, there is a limit to the application of DC biased. Beyond a certain threshold the electrostatic forces overcome the mechanical restoring force, causing the membrane to collapse. This threshold level is referred to as collapse voltage, beyond this point the membrane stops to vibrate. Hence, CMUT is used below the collapse voltage also referred to as pull-in voltage. Other safety and practical issues and low voltage operation also limit the level of applied DC bias voltage. [27].

In ANSYS, for direct coupling of structural and electrostatic domains electromechanical transducer elements called TRANS 126 are used. The spring softening effect can be simulated in ANSYS environment using TRANS 126 element. Collapse voltage was found by performing a static analysis, it came out to be 400Volts. Beyond this value the analysis seized to converge. Although the receive sensitivity is directly proportional to the applied voltage but to avoid electrical breakdown and considering the energy cost, the device is operated in conventional mode. The simulations were performed at 136Volts DC biased that is well within the collapse voltage.

3.1.3: Resonant Frequency:

The membrane's material choice, its geometrical parameters combined with its mass controls the dynamic behavior of the membrane and the frequency characteristics.

A 2D Axisymmetric model was used to perform the Harmonic analysis to investigate the mechanical response of the device as depicted in figure 4 (a). The working frequency of a circular membrane which reflects sensitivity of the proposed structure is highly dependent upon the material properties that are density 'δ', Young's modulus 'E' and Poisson ratio 'v' as indicated by the equation.

$$f = \frac{o.47t_m}{a^2}\sqrt{\frac{E}{p(1-v^2)}}$$

Equation 2: Working frequency of a circular membrane

Initially, a modal analysis was performed to find the workable vibration modes, the maximum center displacement of membrane occurred at the first mode. The modal analysis became precursor for the harmonic analysis to anticipate peak resonance frequency. The peak resonance frequency also know as best working frequency, came out to be 275kHZ.

The resonant frequency at 30%(136V) of the collapse voltage was found by conducting a prestressed harmonic analysis. The best working frequency was estimated to be 264.5kHZ. As our device is intended for underwater communication application, the effects of immersed media on resonant frequency is given by the equation.

$$f_l = \frac{1}{\sqrt{1 + 0.67p_l {}^{R}/_{pt}}}$$

Equation 3: Effects of immersed media on resonant frequency.

The immersion media in our case is water and the resonance frequency is 170kHZ.

The material properties used in the simulations are listed in Table 1.

Table 1: Material Properties

Material	**Youngs Modulus (GPa)**	**Poisson's Ratio**	**Density (kg/m^3)**
Silicon <100>	168	0.22	2330
Silicon Oxide	74.8	0.19	2650

3.2: Final Design Specifications:

Following the analysis and design methodology presented above, a CMUT has been designed and analytically analyzed. Final design specifications of the CMUT are summarized in Table 2.

Table 2: Final CMUT Design Specifications

Parameter	Value
Operating Frequency (kHz)	200
Operating Voltage(V)	136
Resonant Frequency(kHz)	275
Resonant Frequency in Water(kHz)	170
Pull-in voltage(V)	400
Diaphragm thickness(μm)	525
Diaphragm Radius(mm)	2.5
Cavity Height(um)	1

3.3: Receive Sensitivity Analysis:

A CMUT, working in receive mode converts acoustic energy into electrical energy. In response to varying sound pressure, a variable capacitance and voltage appears on the CMUT electrically charged membrane and fixed back plate. In general, output increment caused by per unit input increment or differential of functional relation between input and output is defined as sensitivity. Typically, ratio of electrical output (voltage change) to mechanical input (pressure variation) is referred to as receive sensitivity of the CMUT.

ANSYS 18.1 FEM Package is used to analyze the Finite Element Model. The software enables the acoustic wave propagation by allowing a fluid-structure interaction analysis and allows coupling among displacement degrees of freedom of structural element nodes with displacement degree of freedom of acoustic element nodes.

A transient analysis is performed to find receive sensitivity of designed CMUT device, by transmitting 100kPa wave from a distance of 10ג (lambda) by a flat solid surface working as a piston transducer. The piston is vibrating at an operating frequency of 200kHZ, the pressure wave as a result of this radiating piston strikes the receiving CMUT. A voltage change is sensed across the CMUTs membrane. The recorded voltage per unit change in pressure gives the receive sensitivity of the CMUT. The whole simulation is performed in immersion, water being the immersed liquid.

Element SOLID45 having the capabilities of stress, large deflections, strain and plasticity is the suitable choice for membrane and piston modeling. Immersion medium is modelled by using FLUID30 elements and fluid-structure interaction flags are activated to model fluid-structure interface. Electrostatic transduction on the membrane is achieved by modelling the electrostatic elements using TRANS126. Resistors for reading the generated voltage are modeled by CIRCU124 elements. Silicon material is used as the membrane and Silicon oxide is used as the isolation layer. The physical and material properties are provided in the table 2.

In 3D, a piston transducer identical in dimensions to the designed CMUT is modelled. By applying symmetry boundary conditions around a unit cell, an infinitely large CMUT is assumed. Essentially, a rectangular waveguide with the CMUT at one end and the radiating piston at the other end are modelled. The waveguide is meshed by using FLUID30 elements with the properties of water. The fluid element is given input parameters 1500m/sec as sound velocity and 1000 g/m3 as density. The simplified 2D view of model is depicted in the figure 4, a simplified 2D axisymmetric model of CMUT is presented in figure 4(a), A fixed support is applied at the far end of the CMUT, while the motion at the axis end is constrained only in the x and z direction. The device is allowed to move only in the y direction.

Figure 4(b) showing a piston radiating in a rectangular waveguide and the membrane is placed at the other end. The silicon oxide mimicking the isolation layer was also

included by the radius of the water column. The fluid-structure interface flags were turned on for the surfaces of devices making a contact with the fluid. [28] Transducer element, parallel plate capacitor, are used to model the electrical ports. These TRANS126 elements are used to define the electrode position and electrostatic driving forces. One end of each transducer element is connected to the electrode while the other is connected to 100kohm resistor for measuring the voltage. As applying absorbing boundaries to surfaces other that circular is a taxing job, the involved exercise is avoided by placing the piston and CMUT at 50mm apart and time window for recording the voltage levels is adjusted such that to avoid the first echo. The time window in our case is 33usec to 66usec.

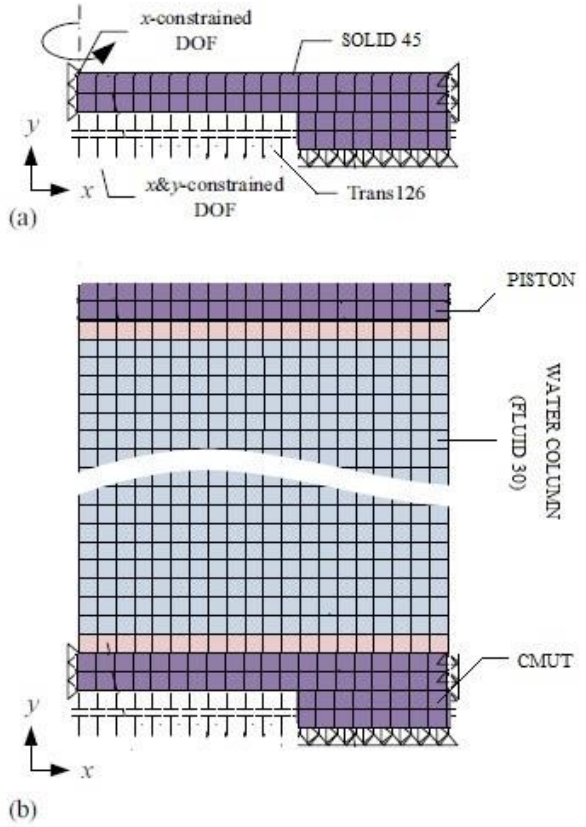

Figure 4: A 2D simplified Model
a) Axisymmetric CMUT with applied boundary conditions
b) Piston transmitting in rectangular waveguide with CMUT at the receiving end.

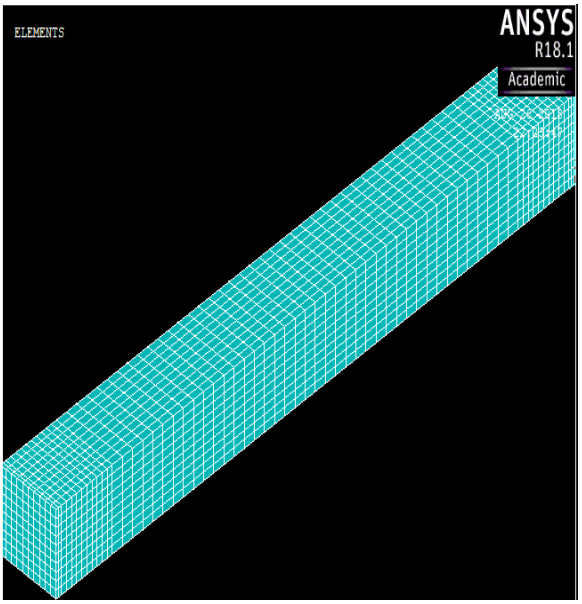

Figure 5: 3D meshed model.

As depicted in the figure (5), to attain high accuracy the mesh is kept denser near and on the piston transducer and CMUT while to decrease processing time the water column is meshed with less density. No of mesh divisions across transducers face is 10 and number of divisions over its thickness is 2.

3.4 Results:

MATLAB software is used to formulate the sensitivity values for the CMUT device.

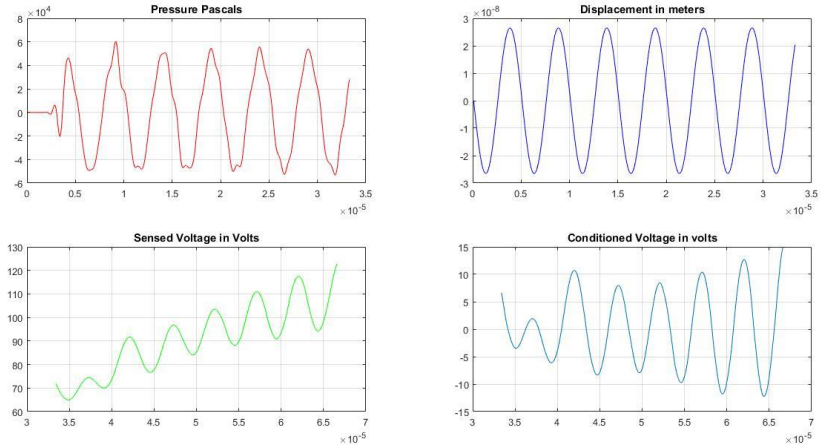

Figure 6: Applied Pressure & displacement and sensed voltage

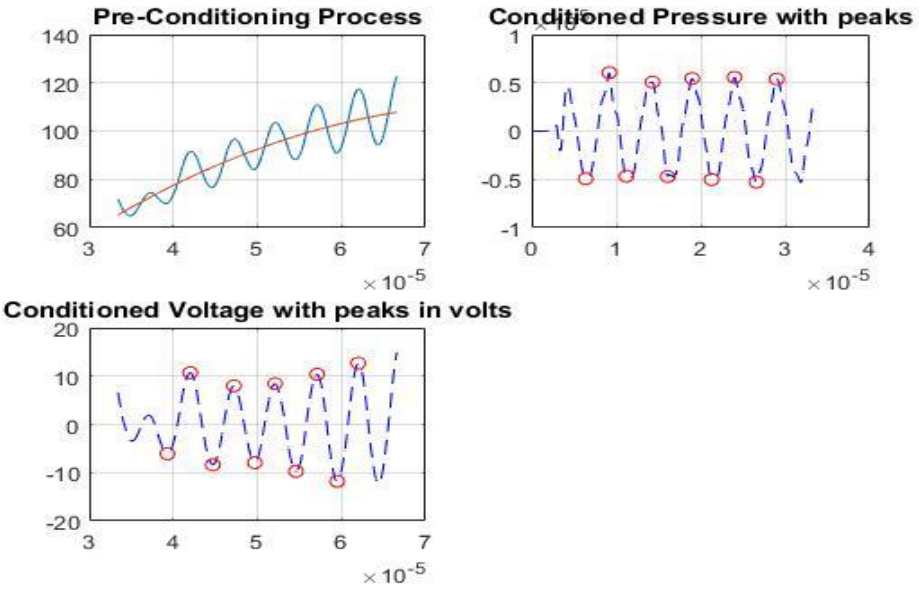

Figure 7: Finding corresponding peaks of pressure and voltage

A piston vibrating @ 200kHz producing a pressure wave of 100kPa placed at 10λ away from the designed CMUT biased with 136volts produces a sensitivity of **-194.8** dB ref (1V/uPa). Various iterations for sensitivity analysis were performed by changing the pressure and applied voltage parameters. The sensitivity for 1.1kPa pressure @ 200kHz for 126Volts biasing gives a sensitivity of **-195dB** ref(1V/uPa). The results are comparable with professional off the shelf available devices such as TC4042 from Reson Teledyne. [34].

CHAPTER 4

FABRICATION:

A CMUT fabrication process based on Au-Au thermocompression wafer-bonding utilizing the complete Si wafer thickness as the membrane, and thermally grown oxide working as the insolation layer is presented next.

The adopted two mask process using Au-Au thermocompression bounding reduces the complexity involved in conventional fabrication process, the alteration in design parameters aims to address and improve device performance as an underwater hydrophone. The detailed description of two mask fabrication is presented in this section.

4.1: Fabrication Process Flow:

A 4-inch boron-doped silicon wafer in <1 0 0> orientation with a thickness of 525 μm and resistivity of 10-20 Ω cm with 1 μm thermally grown oxide layers is used. Single wafer will be used for the fabrication process. After patterning, etching and Au deposition the wafer is spliced in two pairs. The said pairs are bonded by thermocompression process forming a cavity in between. The cavity height is 1 micron and its diameter is kept at 5mm, effectively one half of the pair will act as the bottom fixed electrode and the other half as top electrode utilizing whole of wafer width as the membrane thickness. A lab made thermocompression bonder is used for the bonding purposes.

The parameters of designed CMUT device.

Table 3: Parameters of designed CMUT device.

Parameter	Value
Membrane Radius (a)	2.5mm
Membrane Thickness (t)	525μm
Electrode Radius (a)	2.5mm
Number of Cells	16
Cavity Height (h)	1μm

4.1.1: Mask:

Two chrome on glass masks, designed on layout editor, are used for bonding pads and grooves. Masks are designed to have 2 CMUT devices with 16 cells each.

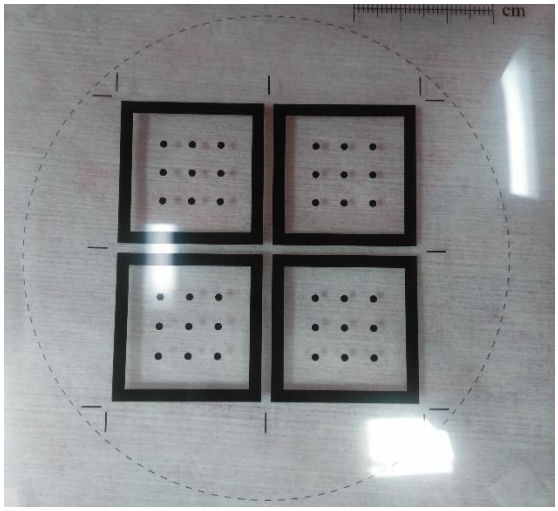

Figure 8: Bonding pads with frame Mask

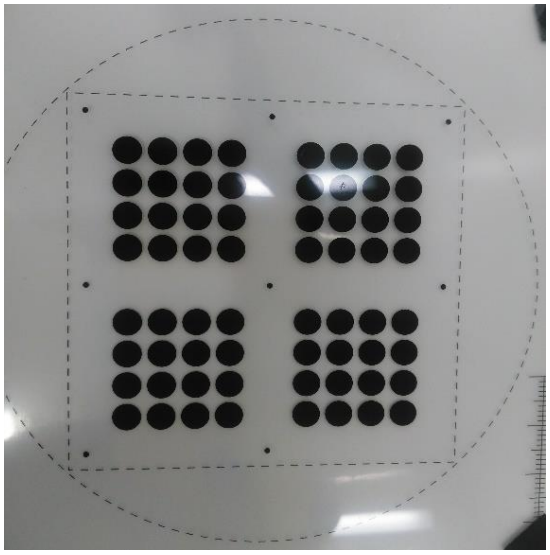

Figure 9: Grooves Mask

The bonding pad mask contains four identical frames for metal deposition with equally spaced 2mm bonding pads falling in the middle of the grooves for firm stiction. The frame with outer dimensions of 30 x 30 mm^2 and is 2.5mm wide. Similarly, the grooves mask contains four arrays of sixteen in number 5mm grooves.

4.1.2: Preparing the wafer:

Before performing any fabrication process on the wafer, it is thoroughly cleaned.

The recipe for wafer cleaning, submerged the wafer in acetone for 5 minutes then keep it in isopropanol for 3 minutes @ 70 C. Rinse the cleaned wafer with copious amounts of DI water and dry it using N2 gun.

4.1.3: Bonding pads and metal layer lithography:

An image reversal Lithography is performed using the bonding pads mask. The negative photolithography process using AZ5214 resist slightly differ from a standard positive resist process: an additional blanket exposure is performed after the initial exposure with a mask, the wafer is baked for a short duration before and after the first exposure. The usual post bake is avoided. After the UV exposure sample is developed in MIF Developer and water is used as the stopper. Rinsing and drying is done by DI and N2 gun.

4.1.4: Metal Au deposition:

After the lithography, the second step includes deposition of Gold (Au) layer, which is the bonding element for our device. Since gold cannot be deposited on Silicon oxide, an adhesion layer of 10nm Chromium is deposited first. After that, 170 nm thick gold layer is deposited using Torr electron-beam evaporator. The wafer is thoroughly cleaned using acetone.

4.1.5: Lithography for Grooves:

A second image reversal lithography step is performed on the sample creating grooves of 5mm diameter. All the Lithography steps are repeated sequentially:

Spin PR Coat, Alignment and Exposure (using Midas / MDA-60MS Mask Aligner 4”), post and prebake after first exposure, flood exposure and development.

4.1.6: Grooves DRIE etching:

After the photo resist removal, 500nm deep cavities are realized by performing Deep Reactive Ion-Etching, DRIE. For etching, Oxford. Plasma lab 100 ICP 300 Deep RIE system is used. The etching parameters are provided in table 4.

Table 4: Etching Parameters.

Parameter	Value
SF6 Flow Rate	45sccm
Chamber Pressure	7.5e-9 Torr
DC Power	50 W
RF Power	2000 W
Etch Rate	2.5nm/sec

4.1.7: Wafer Dicing and preparation for bonding:

After cavity definition, the wafer was spliced into four section using a diamond tip scriber. Before wrapping in Aluminum foils, the four units are carefully aligned at room temperature. The wafers were wrapped in Aluminium foils for protection and uniform distribution of pressure during the bonding process. The bonding procedure is carried out in custom made bonder.

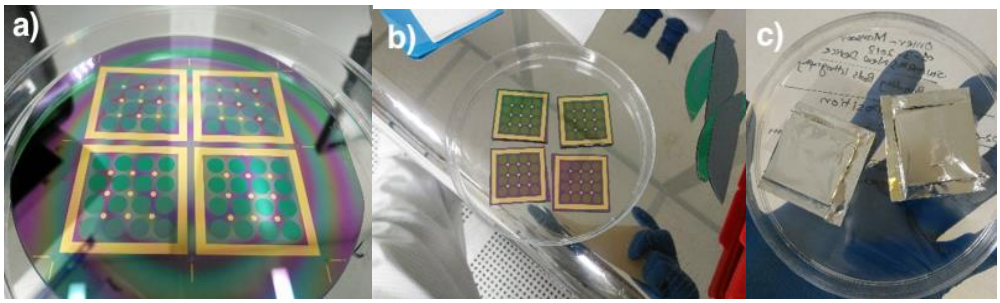

Figure 10 a) Before Dicing; b) After Dicing; c) AI wrapping

4.2: Vacuum thermocompression bonding using custom build bonding tool:

Although, forming Au-Au bond can be a simple and low-cost process. Yet, not much interest has been shown in the field of wafer-level Au thermocompression bonding. Wafer-scale thermocompression bonds with Au using a custom-made bonder has been studied by [29].

For successful bonding the surface smoothness and geometrical flatness of the bonding devices is of great importance. Other parameters that effect the bond quality and strength are temperature and pressure. For gold bonding the temperatures may vary from 100 to 450 ◦C and bonding pressure varies from 0.5 to 120 MPa depending upon the system requirements. Interestingly, the bonding time has less effect on the final bond strength. [30].

The aligned wafer pairs coated in Al foil were bonded in custom-built bonder.

4.3: Bonding equipment:

A thermocompression bonding tool, capable of applying a controlled pressure and temperature across a wafer stack, was constructed. The bonding tool was a purpose-built lab made device. A vacuum pump was used to create vacuum in glass chamber, for complete setup of the bonding tool see figure 11. For uniform transfer of pressure to the wafers, the bond head was constructed with extreme care. Additionally, the wafers to be bonded were placed in an Aluminium foil for uniform pressure distribution.

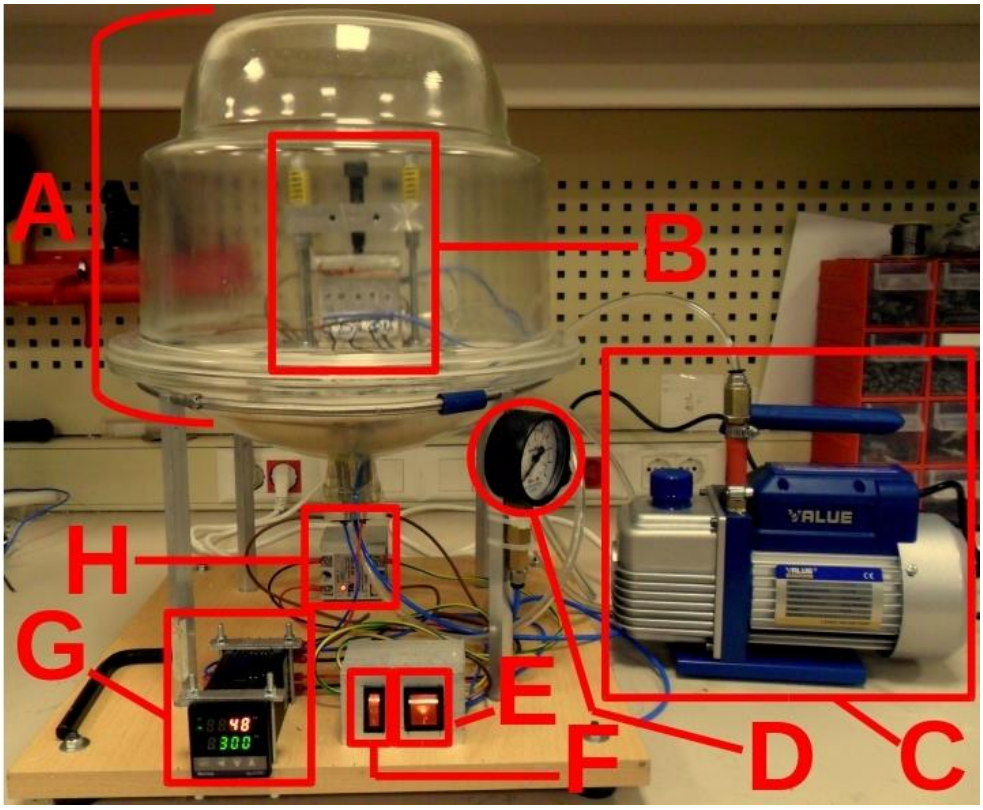

Figure 11: Overall Thermocompression Bonder Setup

(A)Bonding chamber made of inverted desiccator;(B) Bonding element and fixture inside; (C) Pump; (D)Vacuum Gauge; (E) Main power; (F) Heater power; (G)Temperature controller; (H) Relay.

4.3.1: Construction:

An inverted glass desiccator resting on a circular steel bent pipe is maintained by four Aluminium legs, the base of this structure is a wooden frame. An Aluminium fixture serves as the basis for heat insulating ceramic plate, thermal element, wafers pair and compressor element stack. Four auxiliary springs and a compression screw, also supported by the Aluminium, are used for the application of controlled and uniform pressure.

The complete graphic setup representation in Fig. 11 helps to understand the electrical connectivity. Temperature change is monitored and maintained by a PID temperature controller connected to the heating element. For protection the heating element is connected to power switch through a relay. A ¼ HP vacuum pump is used for creating vacuum, pressure change inside the chamber can be monitored by a pressure gauge connected to the main chamber.

The bonding elements are separately shown in Figure 12. The top Aluminium slab (6 cm by 6 cm by 1 cm), metal ball (0.7 cm diameter) along with the compression screw forms the compression elements. The compression elements are insulated from the heating elements by a ceramic slab (6 cm by 6cm by 0.6 cm) attached to the Aluminium slab.

The heating elements are manufactured with two blocks of Aluminium. Each block has the dimension of 6 cm by 6 cm by 2.5 cm. 5 heater elements [31] are inserted into each Aluminium block and sealed with white cement putty as shown in Figure 4(C). The heating elements are insulated again from the Aluminium fixture footing below by another ceramic slab. The temperature sensing is performed by a thermocouple connected to the heating elements from the side of the bonding interface. The pressure gauge valve, pump pipe, thermocouple connection and the electric wires are passed through the opening of the desiccator lid and then sealed with 2-part epoxy. The embodiments are displayed and labeled in Figure 11.

A custom-built calibrated load cell is used for applied pressure measurement. The calibration device is effectively a cantilever. The device is inserted in the Aluminium fixture and the compression screw is turned to get an equivalent electrical voltage measurement.

The voltage steps are calibrated w.r.t kilogram. Evaluation yields that one full turn of the compression screw yields 40-kilogram weight. For the experiments 100-kilogram weight was used for compression which correspond to 2.5 turns of the compression screw.

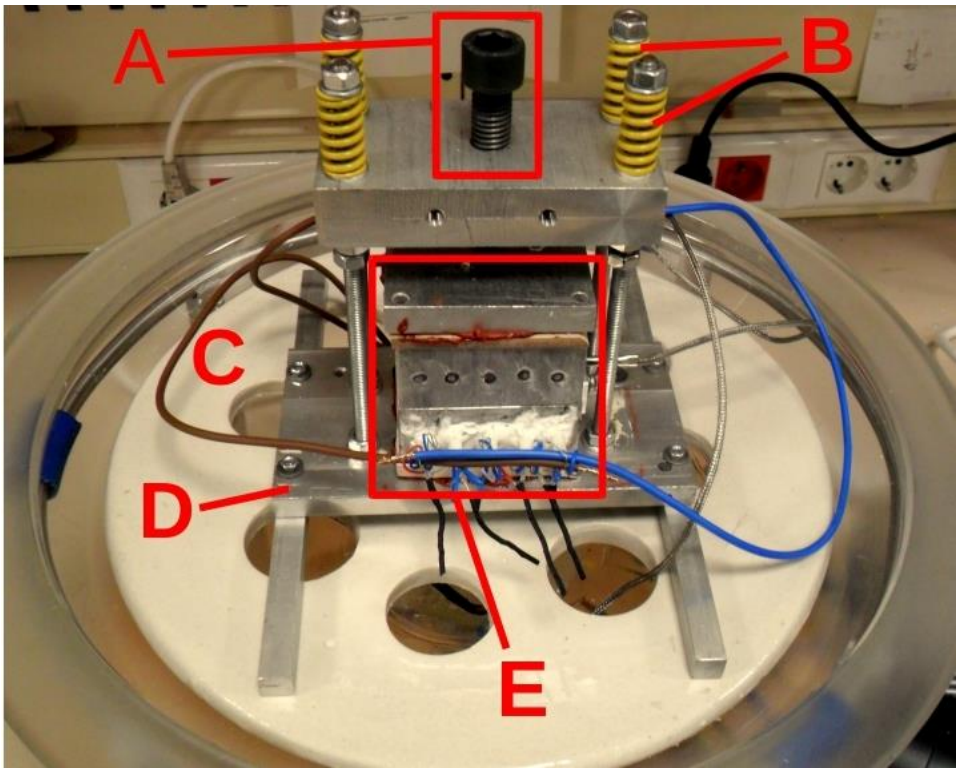

Figure 12: Embodiments inside the Chamber.

(A)Compression screw; (B)Support springs; (C)Supporting ceramic plate; (D)Aluminium fixture for bonding elements; (E)Bonding elements (Thermal and Compression). Thermal elements: Upper & Lower Aluminium block with heating element sealed with white cement.

4.4: Bonding Procedure:

The wafers are bonded on a thermal element with a maximum temperature of 300 °C. The bond temperature is defined as the temperature on the thermal element minus a temperature loss of 2 °C from the Aluminium foil, and a further 2 °C from a silicon wafer. The uncertainty in the given numbers for temperature at the bond interface is estimated to be at most ±4 °C.

After wafer loading, a constant pressure along with a constant temperature is applied during a bonding period of 30 min. A bond pressure of 3.5 MPa was applied. Vacuum is maintained during the complete length of procedure. After bonding, the heating is turned off, but the bond head is not elevated, and pressure is not released until the temperature drops to ~50 °C. The vacuum is released, and the bonded wafers are removed for further action. To enhance the bond strength, two-part epoxy is poured on the edges of the device and is kept in vacuum chamber until the epoxy is cured.

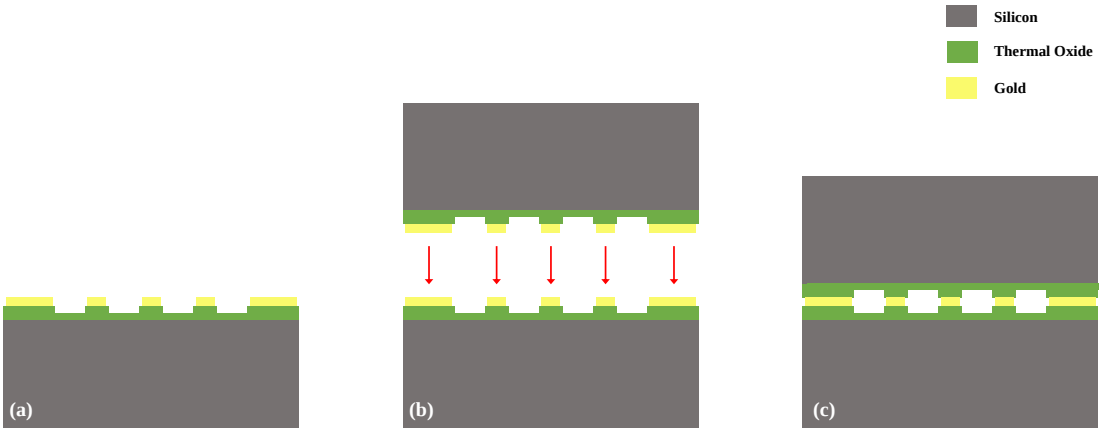

Figure 13: From Sample to Device.

In figure 13 (a) the sample is depicted after patterning, gold deposition and etching. (b) shows the thermocompression bonding process. While the final bonded device is depicted in (c).

Chapter 5:

EXPERIMENTAL CHARACTERIZATION OF THE CMUT:

Before packaging of the devices, a preliminary immersion test is conducted. The transducer prototype is tested in immersion by placing a plastic container around the device and filling the container with sunflower oil (which provides a non-conducting fluid medium with the mechanical properties of water) (Figure 14). The collapse voltage of the device is 400 Volts; hence the applied voltage of 100 Volts (limited by the available power supply) is significantly insufficient for reasonable acoustic coupling.

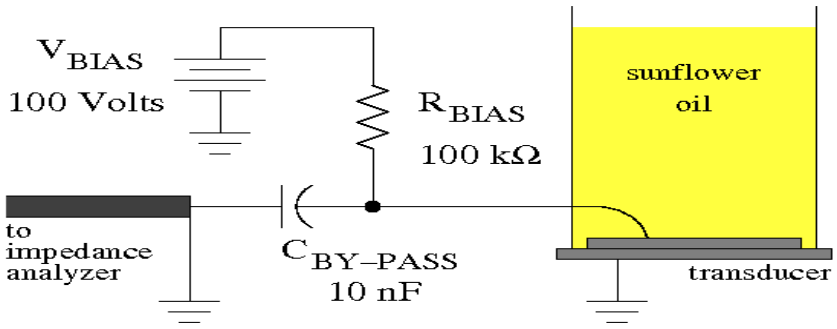

Figure 14: Schematic of Experimental Setup.

To test the change in impedance, the difference between the biased and un-biased measurements was calculated using MATLAB. Poor coupling required averaging to bring out the observable result, which is shown by the solid red curve in Figure14. This initial result indicates that the bandwidth of the transducer is approximately 60 kHz around the center frequency of 175 kHz, with approximately 35% FBW. As expected, fluid loading brought the unloaded resonance frequency down from 275 kHz.

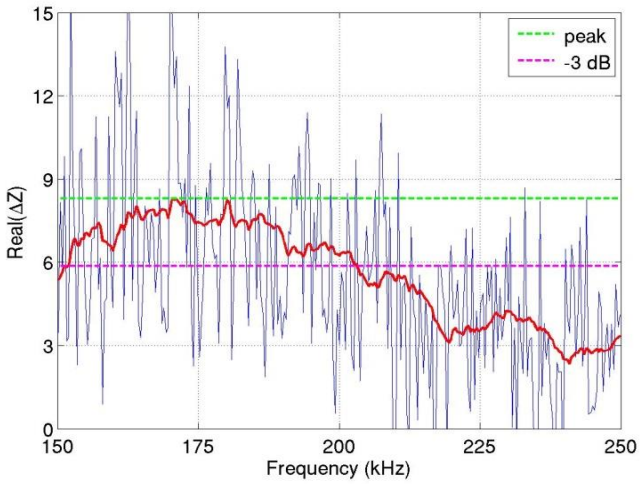

Figure 15: Real part of the radiation impedance for immersed transducer.

5.1: Packaging and preparation for testing:

After the successful preliminary testing the devices are packaged. Two-part epoxy is used to fix the device on an Aluminium slab. The electrical connections are made using the silver epoxy.

Testing fixture is prepared by fixing an extended Aluminium rod with the Al slab. The whole assembly is wrapped in plastic to avoid contact with water.

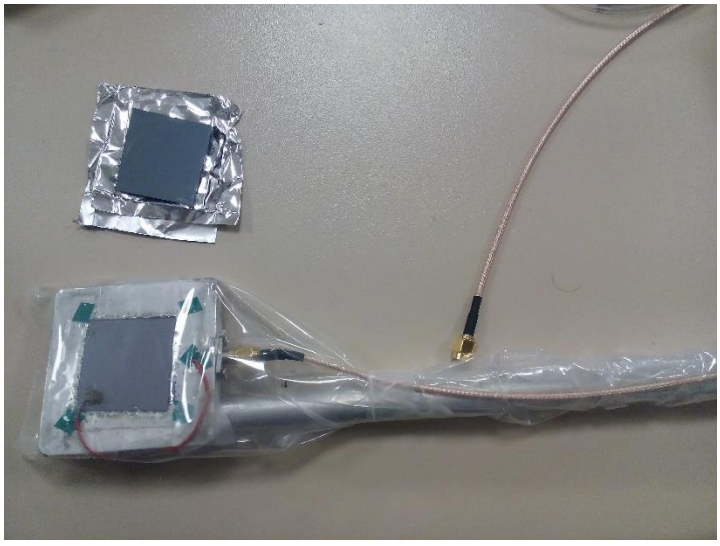

Figure 16: Bonded (top) and packaged device (bottom).

5.2: Receive Sensitivity Experiment:

The experimental setup for characterization of CMUT in receive mode sensitivity is shown in Fig.16. The packaged devices are used for performing the sensitivity tests. [33].

For the experiment a piezoelectric transducer (Valpey Fisher) is used as the transmitter. For determining the output pressure from the transmitter, a 16x16x2.032 mm PZT-5A block is used as the receiver. By using the model in [32], a relationship between measured voltage and received pressure is formed. It is established that a pressure of approximately 2.2kPa produces an equivalent voltage of $40mV_{pp}$ across the face of PZT5A. The properties parameter of PZT piece are given in the table 5. The PZT-5A block has been modeled using Redwood Model in Cadence 6. The circuit schematic for the model is shown in figure 17.

The simulation results in figure 18; shows that for an input force of 1 N (peak) the sensed voltage is observed on the scope screen. The transducer's area is known hence the pressure is calculated to be 3906.25 Pa. The corresponding sensitivity is then 75mV/3906.25Pa, or 19.2uV/Pa. The Mason transformer has a ratio of 1:3.67, and the transducer is a 2mm thick PZT-5A with a working frequency of 1MHz.

The PZT-5A block acts as a calibrated piezo electric hydrophone for measurement of output pressure of the transmitter. The hydrophone is placed at a distance of 95mm from the transmitter. Both the transducer and hydrophone are aligned and immersed in water. A 2cycle burst of $10V_{pp,}$ 200kHz signal from function waveform generator is applied to the transmitter and the output signal is received by the PZT5A block. The corresponding pressure generated by the transmitter is calculated to be 770Pa.

Table 5: Parameters of PZT piece.

Parameter	**Value**
Material	PZT-5A
Thickness	2.032mm
Area	16 X 16
Sound Speed	4350 m/sec
Density	7750 kg/m^3
Resonant Frequency	1 MHz

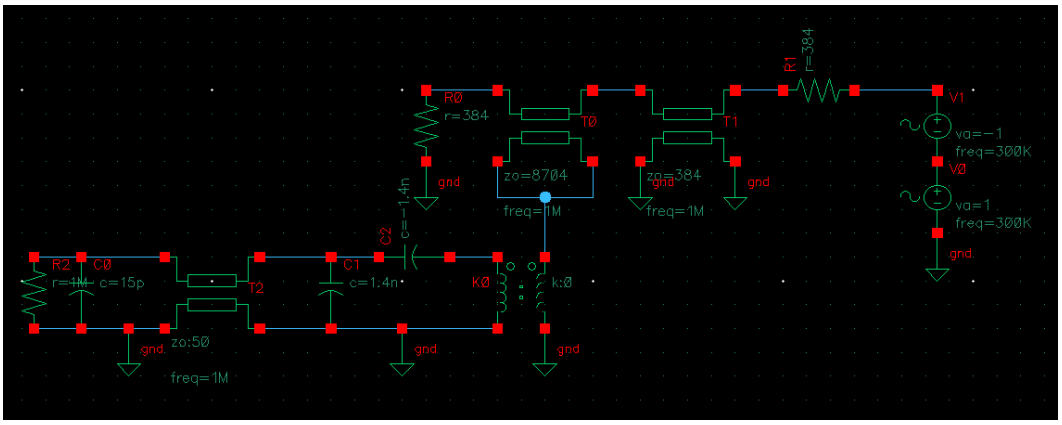

Figure 137: Circuit Schematic for PZT 5A Modeling.

Table 6: List of Components for PZT Circuit

Components	Value
Resistor R_0	384Ω
Resistor R_1	384Ω
Resistor R_2	1MΩ
Capacitor C_0	15pF
Capacitor C_1	1.4nF
Mason Transformer Ratio	1:3.67

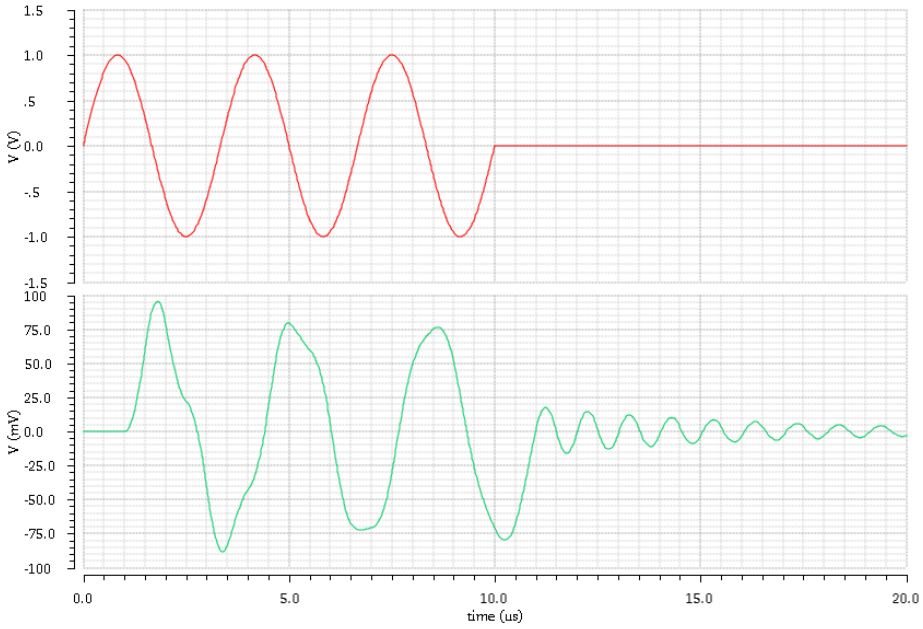

Figure 18: Simulation results for PZT Characterization.

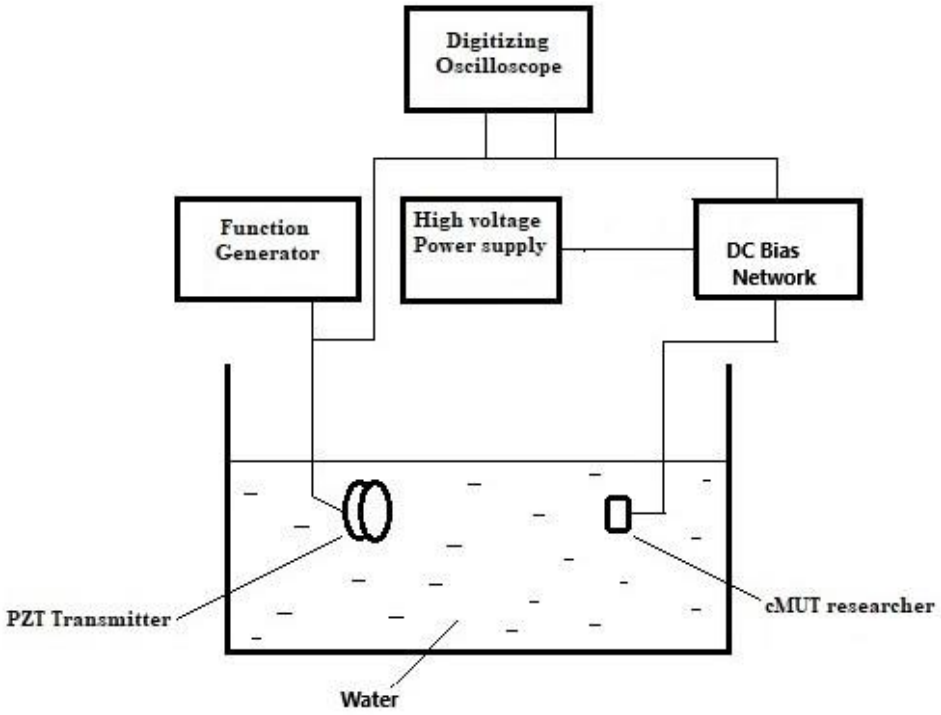

Figure 149: Experimental Setup for CMUT receive sensitivity characterization.

5.2.1: Results:

After recording the generated pressure, the CMUT is placed at the same location, and the DC bias voltage is set at 136 V. The configuration is depicted in figure 19. The received impulse at various frequencies from the CMUT is shown in figure 20.

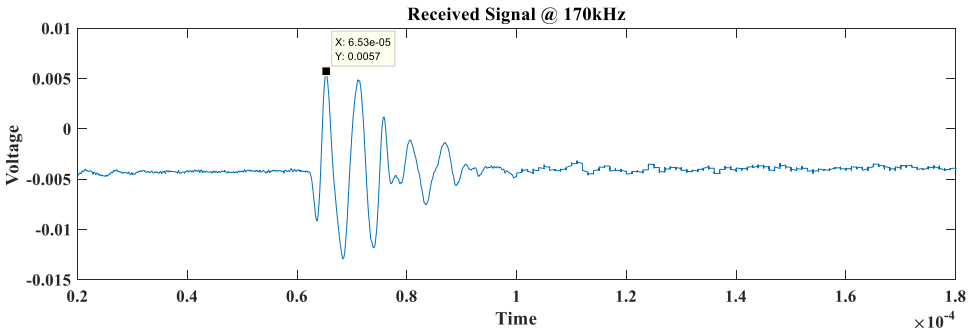

Received Signal at 170kHz

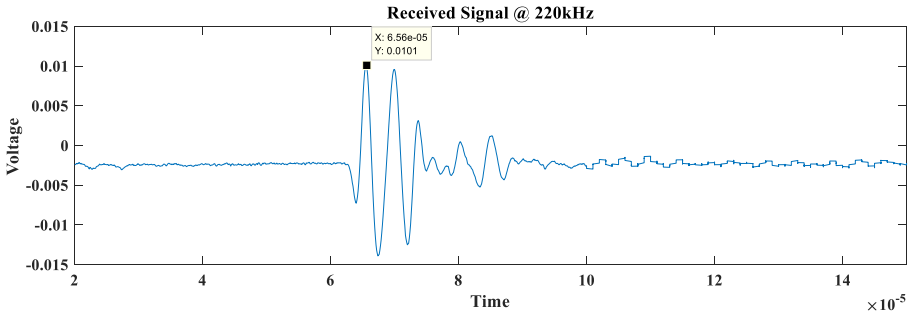

b) Received Signal at 220kHz

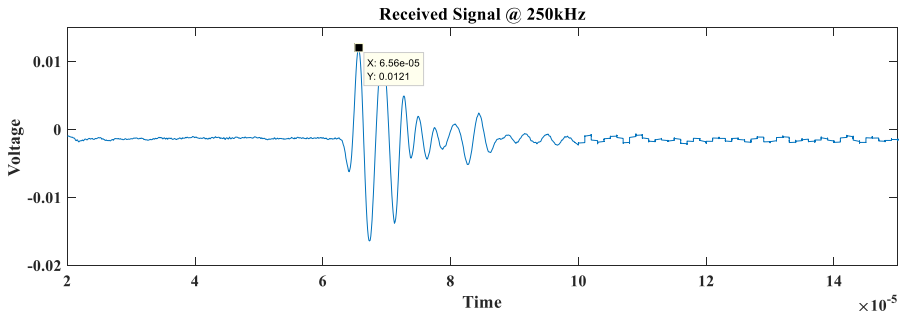

c) Received Signal at 250kHz

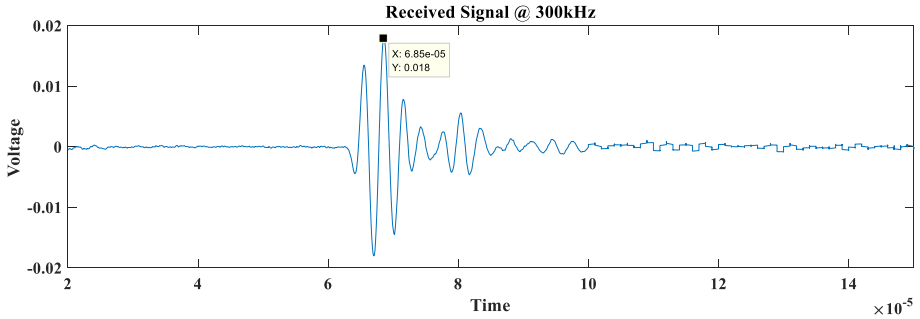

d) Received Signal at 300kHz

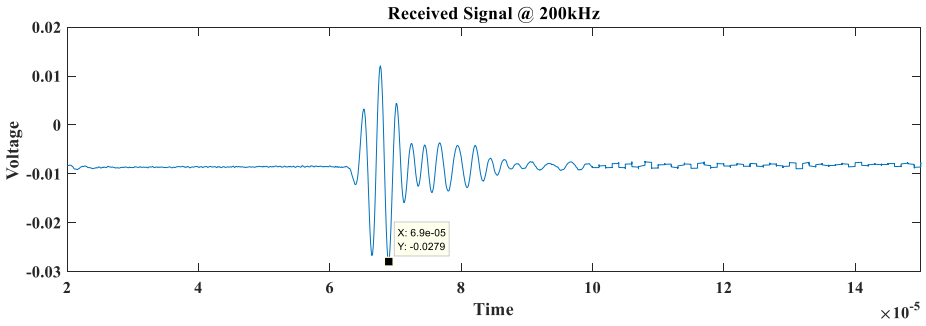

e) Received Signal at 200kHz

Figure 20: Received signals from the CMUT at various frequencies.

a) Received Signal @ 170kHz, b) Received Signal @ 220kHz, c) Received Signal @ 250kHz, d) Received Signal @ 300kHz, e) Received Signal at 200kHz.

The received sensitivity value for the CMUT device is calculated to be **-206dB** ref (1V/uPa). This value is 10dB less than the value earlier calculated with the ANSYS simulation results presented in chapter 3. The nonlinearities caused by the fabrication process and the use of plastic for isolation from water may have caused the variation in the practical results. Furthermore, the assumptions and approximations involved in use of PZT block for calculating the pressure may have also affected the results.

5.3: Frequency Response of CMUTs Receive Sensitivity:

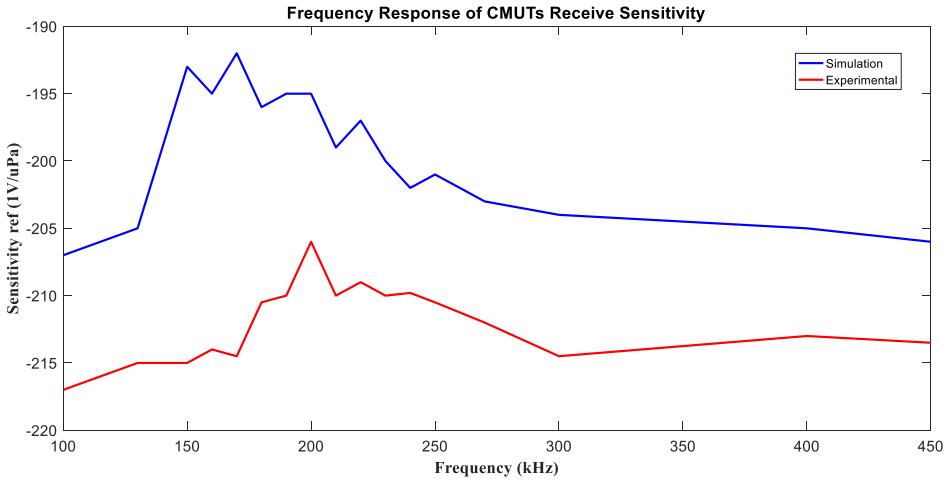

Figure 21: Frequency response of CMUTs Receive Sensitivity.

To neglect the frequency response of transmitter, the receive sensitivity of CMUT is plotted against the frequency. It is clear from the graph that the sensitivity peaks at 200kHz.

To perform the experiment, the CMUT was immersed in water aligned to the transmitter at a distance of 95mm. The experimental setup for receive sensitivity measurement was repeated. The values for pressure calculated from PZT block were measured earlier at frequencies from 100kHz to 400kHz. Similarly, the peak to peak voltages measured by CMUT at frequencies from 100kHz to 400kHz were recorded. Finally, the receive sensitivity was calculated and plotted against the frequency, the CMUT works best as a receiver at and around 200kHz.

Chapter 6:

CONCLUSION & FUTURE WORK:

In this thesis, a comprehensive FEM model for receive sensitivity analysis of CMUT was presented. It was established that CMUTs receive sensitivity can be calculated by performing a transient analysis. By applying symmetry boundary conditions, a unit cell was successfully modeled to depict the complete CMUT.

Although, laboratory testing results of fabricated devices were below than the FEM predicted results. Still we were able to come up with working devices. The fabricated devices were used in SWARMs project and produced acceptable results. In future we plan to strive for bridging the gap between analysis and practical results by improving fabrication and testing procedures. Thus far the focus was on the receive sensitivity parameter of the device. In future, it is aimed to fabricate prototypes with improved compatibility with working environment by addressing the issues such as isolation from water.

References:

[1] A.Quazi and W.Konrad, Underwater acoustic communications, IEEE Comm. Magazine: 24-29, 1982.

[2] L. Liu, S. Zhou and J. Cui, "Prospects and Problems of Wireless Communication for Underwater Sensor Networks," Wiley WCMC Special Issue on Underwater Sensor Networks, 2008.

[3] Sutton J.L. Underwater acoustic imaging. IEEE Proc. 1979; 67:554–566. doi: 10.1109/PROC.1979.11283.

[4] J. H. Goh, A. Shaw, A. I. Al-Shanmma'a, "Underwater Wireless Communication System," Journal of Physics, Conference Series 178, 2009.

[5] S. Bogie, "Conduction and Magnetic Signaling in the Sea," Radio Electronic Engineering, Vol. 42, No. 10, 1972, pp. 447-452. doi:10.1049/ree.1972.0076.

[6] Underwater Acoustic Communication Milica Stojanovic Electrical and Computer Engineering Department Northeastern University Boston, MA 02115.

[7] Underwater Swarm Robotics Review Benjamin T. Champion Deakin University, Matthew A. Joordens Deakin University.

[8] M. A. Joordens and M. Jamshidi, "Consensus Control for a System of Underwater Swarm Robots," Systems Journal, IEEE, vol. 4, pp. 65-73, 2010

[9] Underwater Swarm Networks. Applications, developments, and Medium Access Communication Protocols. Gunilla Elizabeth Burrowes , PhD Thesis, 2014.

[10] Ladabaum I., Khuri-Yakub B.T., Spoliansky D., Haller M.I. Micromachined ultrasonic transducers (MUTs); Proceedings of the 1995 IEEE Ultrasonics Symposium; Seattle, WA, USA. 7–10 November 1995; pp. 501–504.

[11] Eccardt, Niederer, Scheiter, Hierold (Siemens) IUS 1996.

[12] W. Zhang, H. Zhang, F. Du, J. Shi, S. Jin, and Z. Zeng, "Pull-in analysis of the flat circular CMUT cell featuring sealed cavity," Mathematical Problems in Engineering, vol. 2015, Article ID 150279, 9 pages, 2015.

[13] PMUT Royer et al (Honeywell)

[14] Haller & Khuri-Yakub (Stanford) in 1994

[15] A Piezoelectric Micromachined Ultrasound Transducers (pMUT) Array, for Wide Bandwidth Underwater Communication Applications Sina Sadeghpour Paulius Pobedinskas , Ken Haenen and Robert Puers.

[16] Logan and Yeow, 2009; Wang *et al.*, 2014.

[17] Ladabaum et al., 1998.

[18] Cetin and Bayram, 2013.

[19] Zhang et al., 2014.

[20] Logan A and Yeow J T 2009 Fabricating capacitive micromachined ultrasonic transducers with a novel silicon-nitride-based wafer bonding process IEEE Trans. Ultrason. Ferroelectr. Freq. Control 56 1074–84.

[21] Erguri A, Huang Y, Zhuang X, Oralkan Ö, Yarahoglu G G and Khuri-Yakub B T 2005 Capacitive micromachined ultrasonic transducers: fabrication technology IEEE Trans. Ultrason. Ferroelectr. Freq. Control 52 2242–58.

[22] Huang Y, Hæggström E, Badi M H and Khuri-Yakub B 2003 Fabricating capacitive micromachined ultrasonic transducers with wafer-bonding technology J. Microelectromech. Syst. 12 128–37

[23] Yamaner F Y, Zhang X and Oralkan Ö 2015 A three-mask process for fabricating vacuum-sealed capacitive micromachined ultrasonic transducers using anodic bonding IEEE Trans. Ultrasonic. Ferro electronics.

[24] Wafer-level Au–Au bonding in the 350–450 ◦C temperature range Hannah R Tofteberg1, Kari Schjølberg-Henriksen1, Eivind J Fasting2, Alexander S Moen2, Maaike M V Taklo1, Erik U Poppe1 and Christian J Simensen1.

[25] Wafer Bonded Capacitive Micromachined Underwater Transducers Selim Olcum, Kagan Oğuz, Muhammed N. Şenlik, F. Yalçın Yamaner, Ayhan Bozkurt, Abdullah Atalar, Hayrettin Köymen, Bilkent University, Electrical & Electronics Engineering Department, Ankara, 06800 TURKEY 2 Sabancı University, Faculty of Engineering & Natural Sciences, İstanbul, 34956 TURKEY.

[26] Zhuang X. Ph.D. Thesis. Stanford University; Stanford, CA, USA: 2008. Capacitive Micromachined Ultrasonic Transducers with Through-Wafer Interconnects.

[27] Fabrication of Capacitive Micromachined Ultrasonic Transducers (CMUTs) Using Wafer Bonding Technology for Low Frequency (10 kHz150 kHz) Sonar Applications Y. Huang, A. S. Ergun, E. Haeggstrom, and B. T. Khuri-Yakub E. L. Ginaon Laboratory, Stanford University Stanford, CA, 94305-4088.

[28] Finite Element Modeling of Capacitive Micromachined Ultrasonic Transducers. Goksen G. Yaralioglu, Baris Bayram, Amin Nikoozadeh, B.T. Pierre Khuri-Yakub. E.L. Ginzton Laboratory, Stanford University, Stanford, CA 94305.

[29] Strong, high-yield and low-temperature thermocompression silicon wafer-level bonding with gold. M M V Taklo, P Storås, K Schjølberg-Henriksen, H K Hasting and H Jakobsen.

[30] Wafer-level Au–Au bonding in the 350–450 ◦C temperature range Hannah R Tofteberg1, Kari Schjølberg-Henriksen1, Eivind J Fasting, Alexander S Moen, Maaike M V Taklo1, Erik U Poppe1 and Christian J Simensen.

[31] Banggood, Ceramic heater 24v 50w a1322. (Online). https://www.banggood.com/5pcs-24V-50W-A1322-Soldering-Station-Replacement-Heating-Element-Ceramic-Heater-p-1094025.html.

[32] Gordon S. Kino Acoustic Waves: Devices, Imaging, and Analog Signal Processing, Prentice-Hall, 1987.

[33] SIMULATION AND EXPERIMENTAL CHARACTERIZATION OF A 2-D, 3-MHZ CAPACITIVE MICROMACHINED ULTRASONIC TRANSDUCER (CMUT) ARRAY ELEMENT 0. Oralkan, X. C. Jin, F. L. Degertekin, and B. T. Khuri-Yakub Edward L. Ginzton Laboratory.

[34] TC4042 Low-Noise Spherical Hydrophone by Teledyne RESON.

[35] http://www.swarms.eu/Smart and networking underwater robots in cooperation meshes.